

# Identifying true satellites of the Magellanic Clouds

Laura V. Sales<sup>1\*</sup>, Julio F. Navarro<sup>2</sup>, Nitya Kallivayalil<sup>3</sup> and Carlos S. Frenk<sup>4</sup>

<sup>1</sup> *Department of Physics and Astronomy, University of California Riverside, 900 University Ave., CA92507, US*

<sup>2</sup> *Senior CIFAR Fellow. Department of Physics and Astronomy, University of Victoria, Victoria, BC V8P 5C2, Canada*

<sup>3</sup> *Department of Astronomy, University of Virginia, Charlottesville, VA 22904, USA*

<sup>4</sup> *Institute for Computational Cosmology, Department of Physics, University of Durham, South Road, Durham DH1 3LE, UK*

13 May 2016

## ABSTRACT

The hierarchical nature of  $\Lambda$ CDM suggests that the Magellanic Clouds must have been surrounded by a number of satellites before their infall into the Milky Way. Many of those satellites should still be in close proximity to the Clouds, but some could have dispersed ahead/behind the Clouds along their Galactic orbit. Either way, prior association with the Clouds results in strong restrictions on the present-day positions and velocities of candidate Magellanic satellites: they must lie close to the nearly-polar orbital plane of the Magellanic stream, and their distances and radial velocities must follow the latitude dependence expected for a tidal stream with the Clouds at pericenter. We use a cosmological numerical simulation of the disruption of a massive subhalo in a Milky Way-sized  $\Lambda$ CDM halo to test whether any of the 20 dwarfs recently-discovered in the DES, SMASH, Pan-STARRS, and ATLAS surveys are truly associated with the Clouds. Of the 6 systems with kinematic data, only Hydra II and Hor 1 have distances and radial velocities consistent with a Magellanic origin. Of the remaining dwarfs, six (Hor 2, Eri 3, Ret 3, Tuc 4, Tuc 5, and Phx 2) have positions and distances consistent with a Magellanic origin, but kinematic data are needed to substantiate that possibility. Conclusive evidence for association would require proper motions to constrain the orbital angular momentum direction, which, for true Magellanic satellites, must coincide with that of the Clouds. We use this result to predict radial velocities and proper motions for all new dwarfs. Our results are relatively insensitive to the assumption of first or second pericenter for the Clouds.

**Key words:** galaxies: haloes - galaxies: formation - galaxies: evolution - galaxies: kinematics and dynamics.

## 1 INTRODUCTION

The Large and Small Magellanic Clouds (LMC and SMC, respectively) are a galaxy pair orbiting together in the halo of the Milky Way and provide a prime example of the nested hierarchy of structures expected in the  $\Lambda$ CDM galaxy formation paradigm (Springel et al. 2008). Their physical association seems beyond doubt, given their relative proximity, correlated kinematics, and abundant evidence of past interaction (for a recent review, see, e.g., D’Onghia & Fox 2015).

The path of the Clouds around the Galaxy is well constrained by precise estimates of their distances, positions, radial velocities and proper motions, which indicate a nearly-polar orbit on a plane closely aligned with the Magellanic Stream (Kallivayalil et al. 2006). The Clouds are just past pericenter, since their Galactocentric radial velocities are positive and much smaller than their

tangential velocities ( $V_t \sim 314$ ,  $V_r \sim +64$  km/s for the LMC, see, e.g., Kallivayalil et al. 2013). Their orbit must also have a fairly large apocentric radius, since their total speed ( $|V_{\text{LMC}}| \sim 321$  km/s) exceeds the circular velocity of the Milky Way ( $\sim 220$  km/s) by a substantial amount. A large apocenter implies a long orbital period, which has led to the suggestion that the Clouds might be on their first pericentric passage.

This conclusion depends on the total mass assumed for the Milky Way halo, as well as on its assumed outer radial profile (Besla et al. 2007), but it would explain naturally why the LMC and SMC are still so tightly bound. Indeed, if the Clouds were at first pericenter then the Galactic tide would not have yet had time to disrupt the pair nor to disperse fully the common (sub)halo they inhabit. As a result, most other dwarf companions of the Clouds should still lie in their close vicinity. Such “Magellanic satellites” have long been speculated (see, e.g., Lynden-Bell & Lynden-Bell 1995), and their existence would be consistent with the relatively common occurrence of dwarf galaxy associations in the nearby

\* E-mail: lsales@ucr.edu

Universe (Tully et al. 2006). The immediate surroundings of the Clouds should thus be a fertile ground to search for new dwarfs, as proposed by Sales et al. (2011, S11 hereafter).

A full search for satellites around the Clouds would be extremely valuable. One reason is that, in  $\Lambda$ CDM, the satellite luminosity function is expected to be a nearly scale-free function when expressed in units of the luminosity of the primary (Sales et al. 2013). In other words, to first order, the Galactic satellite abundance should be simply a scaled-up version of that of the Clouds. A complete catalogue of Magellanic faint and ultra-faint satellites would be easier to compile (the relevant survey volume is much smaller than the full Galactic halo) and could therefore help to constrain the incompleteness of all-sky surveys of Galactic satellites. In general, the surrounding of dwarf galaxies, especially those in the field, are promising sites for the discovery of new faint galaxies (Sales et al. 2013; Wheeler et al. 2015).

A second application would be to clarify the effects of environment on the star formation history of dwarfs (D’Onghia & Lake 2008; Wetzel et al. 2015). An unambiguous identification of Magellanic origin would enable a direct comparison with Galactic satellites of similar stellar mass that have evolved in a rather different environment. Finally, Magellanic satellites might also provide clues to the nature of dark matter: indeed, fewer satellites are expected around the Milky Way in general, and the LMC in particular, if dark matter was “warm” rather than cold (see, e.g., Kennedy et al. 2014).

Given this context, it is not surprising that the recent discovery of a number of candidate dwarfs in southern surveys targeting the Clouds’ vicinity, such as the Dark Energy Survey (DES; Bechtol et al. 2015; Koposov et al. 2015; Drlica-Wagner et al. 2015; Kim & Jerjen 2015; Kim et al. 2015), the Survey of the Magellanic Stellar History (SMASH; Martin et al. 2015), as well as in other large surveys, such as PAN-STARRS (Laevens et al. 2015), and ATLAS (Torrealba et al. 2016), have attracted much attention.

While not all of these candidates have follow-up spectroscopy confirming that they are dark matter-dominated dwarf galaxies rather than star clusters—six have spectra thus far (Walker et al. 2016; Kirby et al. 2015; Martin et al. 2016)—they do occupy the same region in the size-luminosity plane as ultra-faint dwarf galaxies ( $M_V$  between  $-2.0$  and  $-7.8$  and half-light radii,  $r_h$ , between  $\sim 18$  and  $\sim 1000$  pc). It is not clear either which of these dwarfs, if any, have a Magellanic origin.

On that point, Deason et al. (2015) cite a statistical argument based on abundance-matching models applied to massive subhalos in the ELVIS simulations (Garrison-Kimmel et al. 2014) to suggest that 2-4 of the 9 then known DES candidates might have come into the Milky Way with the LMC. Yozin & Bekki (2015), on the other hand, conclude, on the basis of orbit models, that the majority of the DES dwarfs could have been at least loosely associated with the Clouds. Yet another analysis suggests, using tailor-made numerical simulations, that only about half of the DES new dwarf galaxies are very likely to have been associated with the LMC in the past (Jethwa et al. 2016).

Here, we take a complementary and targeted approach, using an LMC analog subhalo identified in a fully cosmological simulation of a Milky Way-sized halo in  $\Lambda$ CDM. We track the positions and velocities of subhalo particles to constrain the likely location in phase space of systems with prior association with the Clouds. This is an extension of the analysis previously presented in S11, who concluded that *none* of the 26 Milky Way satellites known at the time were convincingly associated with the Clouds. The main goal of the present work is to assess the likelihood of association

with the Clouds of the recently-discovered dwarfs, as well as to predict the radial velocities and proper motions required for that association to be true.

In § 2 we describe our numerical set up, in § 3 we present the main results, including the expected sky distribution of the companion dwarfs, their radial velocities, probability of association with the LMC, as well as their 3D orbits. We conclude with a brief summary of our main conclusions in § 4.

## 2 NUMERICAL SIMULATIONS

We use the Aquarius Project (Springel et al. 2008), a suite of zoomed-in cosmological simulations that follow the formation of 6 Milky Way-sized halos with virial<sup>1</sup> masses in the range  $0.8\text{--}1.8 \times 10^{12} M_\odot$ . These halos were selected from a large scale simulation of a cosmologically representative volume (the Millennium-II Simulation, see Boylan-Kolchin et al. 2009). We focus in this paper on the properties of an “LMC analog” system (hereafter identified as LMCa, for short) which was identified and presented in S11.

### 2.1 LMCa: the LMC analog

LMCa was chosen because it is a fairly massive subhalo with a pericentric distance ( $\sim 50$  kpc) and velocity ( $\sim 400$  km/s) in good agreement with that of the LMC (Kallivayalil et al. 2006, hereafter K06). Identified before infall, at  $z_{id} = 0.9$ , LMCa has a virial mass of  $M_{200} = 3.6 \times 10^{10} M_\odot$ , which corresponds to a circular velocity of  $\sim 65$  km/s.

LMCa first crosses the virial boundary of the main Aquarius halo (Aq-A) at  $z = 0.51$  ( $t = 8.6$  Gyr), reaches first pericenter at  $t_{1p} = 9.6$  Gyr, and is able to complete a second pericentric passage at  $t_{2p} = 13.3$  Gyr. The host halo has a virial mass of  $M_{200} = 1.8 \times 10^{12} M_\odot$  at  $z = 0$ . (These times are actually slightly past actual pericenter, thus chosen so as to best accommodate the fact that the LMC has a slight positive radial velocity and is itself just past pericenter at present.)

At  $t_{1p}$  and  $t_{2p}$ , the distances, radial velocities, and tangential velocities are, respectively,  $r_{1p} = 65$  kpc,  $r_{2p} = 69$  kpc,  $V_{r,1p} = 78$  km/s,  $V_{r,2p} = 89$  km/s;  $V_{t,1p} = 345$  km/s; and  $V_{t,2p} = 302$  km/s. These values are in reasonable agreement with the K06 LMC measurements (see Fig. 1 in S11), although the tangential velocities were a bit below the observed values. The revised proper motions for the LMC from Kallivayalil et al. (2013) suggest a slightly lower total velocity than previously determined,  $321 \pm 24$  km/s compared to  $378 \pm 31$  km/s, resulting from the combination of an added third-epoch of observations, the adoption of a different local standard of rest, and a new determination of the LMC’s dynamical center. This decrease in velocity accommodates the tangential motion of LMCa more comfortably at both pericenters.

It is still a matter of debate whether the Clouds are on first or second pericentric passage (see, e.g., Shattow & Loeb 2009; Sales et al. 2011), although indirect evidence favour a first infall scenario, including: *a*) their large tangential velocity, *b*) their blue colors and

<sup>1</sup> We define the virial mass,  $M_{200}$ , as that enclosed by a sphere of mean density 200 times the critical density of the Universe,  $\rho_{crit} = 3H^2/8\pi G$ . Virial quantities are defined at that radius, and are identified by a “200” subscript.

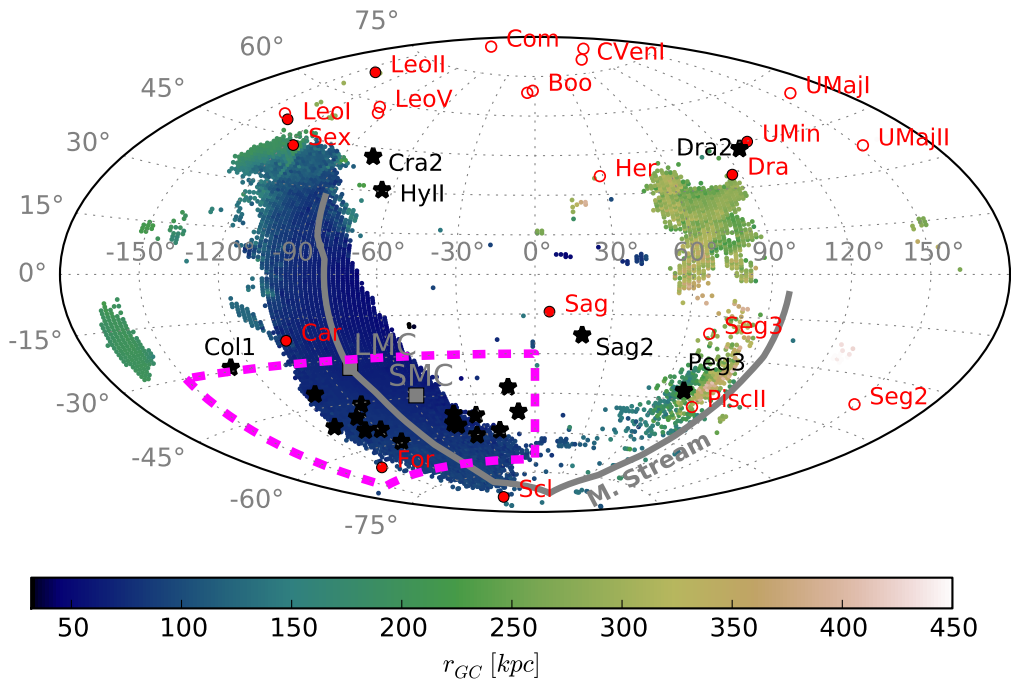


**Figure 1.** Aitoff projection of particles associated with the LMC analog subhalo (LMCa), shown just after first pericentric approach, when its pericentric distance and velocity closely matches that of the Large Magellanic Cloud. The LMCa center is chosen to coincide with the LMC and coordinates are chosen so that the direction of its orbital angular momentum matches that of the LMC. This results in a nearly-polar orbital plane, which roughly aligns with the Magellanic Stream (grey line). Particles of the LMC analog (identified before infall) are colored by their average Galactocentric distance. Red circles indicate the position of known Milky Way satellites. Filled circles indicate “classical” dwarf spheroidals (i.e., brighter than  $M_V = -8$ ); open circles denote fainter objects. Newly discovered dwarfs (the subject of this paper) are shown as black starred symbols.

large gas content and *c*) the requirement that the LMC and SMC have been a long-lived binary (which favors a low-mass Milky Way, or a high-mass LMC, see discussion in [Kallivayalil et al. 2013](#)). Therefore in what follows we analyze in detail a first infall scenario but include a brief discussion about how our conclusions would be affected if the LMC is in its second pericenter passage (Sec. 3.5).

Following S11, we use the Aquarius “A” halo at level 3 resolution, or Aq-A-3 in the notation of [Springel et al. \(2008\)](#), which has a mass per particle  $m_p = 4.9 \times 10^4 M_\odot$ . We identify and follow all particles that were associated with the LMCa friends-of-friends group at the time of infall, and evaluate their positions and velocities at the time of first and second pericenter passages.

Using SUBFIND (Springel et al. 2001), we have identified more than 200 subhalos associated with LMCa at infall time (see Fig. 1 in S11 for their individual orbits), suggesting that a large satellite such as the LMC should bring along its own population of satellites (Springel et al. 2008). We use for our analysis *all* particles (and not just the subhalos) initially bound to LMCa in order to provide a more complete sampling of the positions and velocities of any potential companion associated with the LMC.

LMC. For consistency with S11, we use throughout this paper the LMC proper motion as given by K06<sup>2</sup>. After the rotation, we also rescale slightly all Galactocentric distances so that LMCa is, at each pericenter, at the measured distance of the LMC: 49 kpc.

### 3 RESULTS

We first examine the sky distribution of particles associated at infall with the LMC analog subhalo (hereafter “LMCa debris”, for short). We use this footprint, as well as their radial and tangential velocities, to compare with available data for the newly-discovered dwarfs. As mentioned above, we shall interpret coincidence in sky position, radial velocity and distance between debris particles and observed dwarfs as evidence of a possible association with the LMC.

## 2.2 LMCa in Galactic coordinates

We transform the coordinate system of the simulation into “Galactic coordinates” by requiring that the orientation of the orbital angular momentum of LMCa coincides with that measured for the LMC’s orbit, and that its position on the sky coincides with the

<sup>2</sup> We note however that the change in the direction of the orbit given by the new updated measurements from Kallivayalil et al. (2013) is very small:  $(j_x, j_y, j_z) = (-0.97, 0.14, -0.18)$  versus  $(-0.98, 0.11, -0.13)$  for the 2006 and 2013 determinations, respectively. These numbers correspond to a unit vector in a Cartesian system aligned with the disk of the galaxy, as described in Sec. 3.

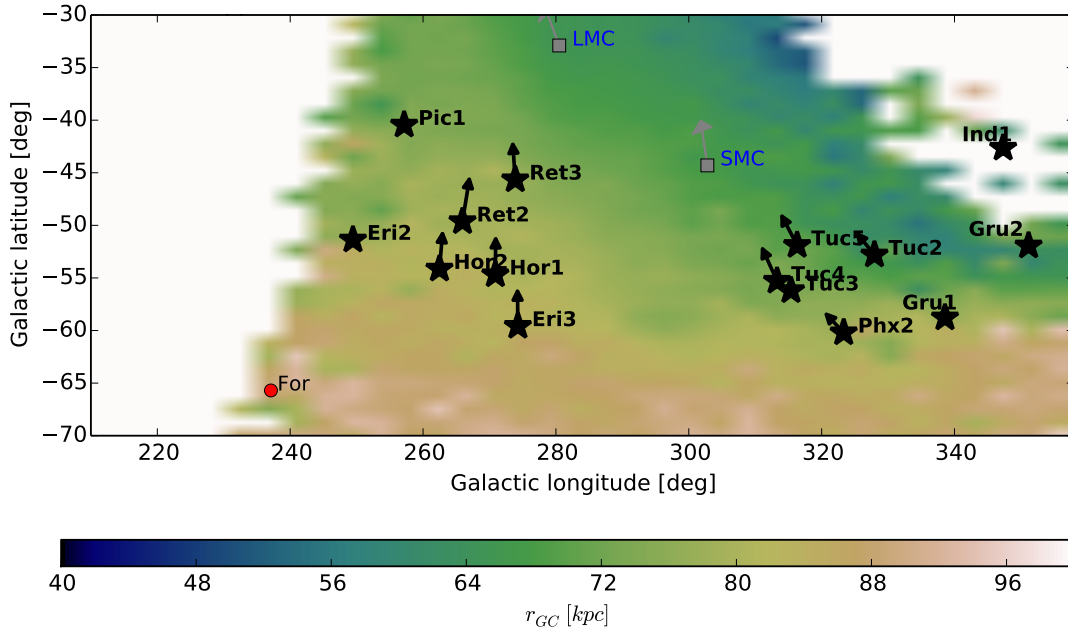


**Figure 2.** Zoom-in of the area just south of the Clouds outlined by the dashed magenta box in Fig. 1. This area samples the trailing arm of the LMCa tidal debris, and contains the new dwarfs discovered in the Dark Energy Survey (DES). Col 1 is the only DES dwarf located far away from the stream (not shown). Note also that Ind 1 has now been shown to be a star cluster (Kim et al. 2015). The LMC and SMC are shown as grey squares; red circles are previously known Galactic satellites; new dwarfs are shown by starred symbols. The arrows indicate the expected tangential motion of those satellites, assuming that they were associated with the Clouds (see Sec. 3.6). Arrows are only shown for systems deemed likely Magellanic satellite candidates in a first pericenter passage scenario (see text for more details).

### 3.1 LMCa debris: sky distribution and distances

At the time of the first pericenter, tidal disruption due to the host halo has already set in, but most particles are still bound and close to the subhalo center. The rest of the material is distributed along a thick but well-defined tidal stream that follows the projection of the subhalo’s orbital path on the sky. A leading and trailing arm extend towards more positive and negative latitudes, respectively. The distribution of this debris roughly agrees with the position of the HI Magellanic Stream, sketched here by a line that traces the high-density HI in the sky maps of Nidever et al. (2010).

Most of the debris, however, is close to the current position of the Clouds (grey squares indicate the observed positions of the LMC and SMC). Particles are colour coded in Fig. 1 by their Galactocentric distance (see color bar), which shows a clear gradient along the stream with distances reaching up to 300 kpc, well beyond the virial radius of the main host.

For reference, we indicate the positions of all known Milky Way satellites in the figure as well. Red filled circles correspond to the “classical” (i.e., brighter than  $M_v = -8$ ) dwarf spheroidal (dSph) companions of the Milky Way; open circles indicate the position of previously known, fainter satellites. We refer the interested reader to S11 for a discussion of the probability of association with the LMC of those satellites.

The recently-discovered dwarfs that are the focus of this paper are shown using black starred symbols in Fig. 1. We include in this sample: (i) the dwarfs reported by Koposov et al. (2015) from year-1 DES data (see also Bechtol et al. 2015), (ii) the 6 certain detections from year-2 DES data (Drlica-Wagner et al. 2015), and (iii) additional individual discoveries such as Hydra II (Martin et al. 2015, Hy II), Horologium 2 (Kim & Jerjen 2015, Hor 2), Pegasus 3

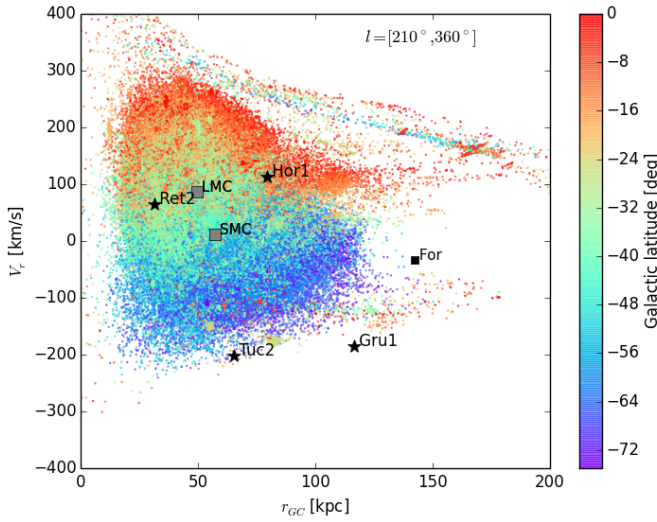
(Kim et al. 2015, Peg 3), Draco 2 and Sagittarius 2 (Laevens et al. 2015, Dra 2 and Sag 2) and Crater 2 (Torrealba et al. 2016, Cra 2). Table 1 lists all the “new dwarfs” considered in what follows (i.e., black stars in Fig. 1). With the exception of Hy II, Cra 2 and Dra 2, all other dwarfs are in the region of the sky occupied by the trailing arm of the stream.

Fig. 1 shows that position on the sky and distance provide on their own powerful constraints on a potential Magellanic origin for a dwarf. Those satellites must be close to the orbital plane (traced by the debris and the Magellanic Stream), ruling out satellites like Sagittarius, Hercules, and Seg 2. In addition, the farther a satellite is from the LMC the larger, on average, its Galactocentric distance should be, a fact that rules out many of the satellites in the Galactic northern cap. Indeed, the latter are typically much closer to the Galactic centre than the leading arm of the LMCa debris, which reaches a distance of  $\sim 180$  kpc at  $b = +45^\circ$ .

Fig. 2 zooms in on the vicinity of the LMC (the region highlighted by the magenta box in Fig. 1) and shows in more detail the position of individual dwarfs as well as the distance gradient expected for this section of the stream. This figure also shows that Col 1 lies outside of the LMCa debris footprint. This, combined with its large distance ( $\sim 182$  kpc) makes a Magellanic association rather unlikely (see also Drlica-Wagner et al. 2015). We therefore exclude Col 1 from the rest of our analysis, together with Sag 2, whose position in the sky is not favorable either. Furthermore, we also remove Indus 1 from our analysis since it has now been classified as a stellar cluster rather than a dwarf galaxy (Kim et al. 2015).

The distance gradients with Galactic latitude shown in Figs. 1 and 2 result from the fact that LMCa is close to pericenter and,





**Figure 3.** Galactocentric distance  $r_{GC}$  vs. radial velocity  $V_r$  for LMCa particles at first pericenter, color-coded by Galactic latitude  $b$  ( $-80^\circ < b < 0^\circ$ ; see color bar on right). For clarity, we only show the Galactic longitude range  $l = [210^\circ, 360^\circ]$ , which encompasses most of the LMCa material in Fig. 1. Note the correlation between latitude and radial velocity, with the leading arm having already passed through pericenter (positive  $V_r$ ) and the trailing material still approaching the Galaxy with  $V_r < 0$ . As before, the LMC and SMC are shown with grey squares and other previously known dwarfs in this region of the sky are marked with black squares; new dwarfs with measured kinematics are shown with black starred symbols. The little overlap between Fornax, Gru 1 and Tuc 2 and the LMCa debris implies a low probability of prior association between these dwarfs and the LMC, assuming first infall. Hor 1 is the dwarf most likely to have had a Magellanic association.

therefore, at roughly the minimum distance of all associated debris. Debris north of the LMC is farther away and moving out (already past pericenter), whereas debris to the south is also farther away but moving in (has yet to reach pericenter). This induces a correlated signature in the radial velocities, which we explore next.

### 3.2 LMCa debris: radial velocities

We explore the correlation between radial velocity and Galactic latitude in Fig. 3. This figure shows the Galactocentric radial velocity  $V_r$  as a function of distance  $r_{GC}$  for LMCa debris in the Galactic longitude range  $l = [210^\circ - 360^\circ]$ , which encloses the stream and the positions of the DES dwarfs.

Particles are colored according to their Galactic latitude, in the range  $-80^\circ < b < 0^\circ$  (see color bar). Fig. 3 shows a clear gradient in radial velocity with Galactic latitude, showing generally positive values (outward moving) for particles north of the position of the LMC (i.e.,  $b_{LMC} > -32.9^\circ$ ) and negative values (in-falling) for those south of that. Although the latitude trend is clear, the dispersion about the mean trend is quite large. This is because the velocity dispersion of LMCa before infall was quite substantial (at  $z_{id} = 0.9$ ,  $\sigma_{200} = V_{200}/\sqrt{2} = 44.5$  km/s), making the tidally-induced stream quite thick. As a result, the constraints on a possible Magellanic origin provided by  $b$ ,  $r_{GC}$  and  $V_r$  alone are relatively lax, and serve mainly to rule out the most unlikely candidates.

For example, Fig. 3 shows that Fornax (even though it is close

to the stream in sky projection) has a distance that is too large to be associated with the LMC, whereas the SMC, as expected, lies well within the velocity-distance range spanned by the LMCa debris. Starred symbols show the “new dwarfs” that fall in this region of the sky and for which kinematic measurements are available (Walker et al. 2016; Koposov et al. 2015): Hor 1, Ret 2 are clear candidates, whereas Tuc 2 and Gru 1 seem only marginally consistent with a Magellanic origin.

More stringent constraints may be obtained by combining the results from Fig. 1 and Fig. 3, since membership to the LMC group is only likely for systems in narrow regions of the four dimensional space drawn by (i) position on the sky ( $l, b$ ); (ii) radial velocity  $V_r$ , and (iii) Galactocentric distance  $r_{GC}$ . We illustrate this in Fig. 4, where we plot the distance and radial velocity of all LMCa particles whose positions on the sky fall within  $5^\circ$  of each individual dwarf.

The top two panels on the left of Fig. 4 are meant to illustrate the analysis procedure. For the case of the LMC (top left) most particles in the LMCa subhalo are, by construction (Sec. 2.2), at the observed location and radial velocity of the LMC (shown with a blue square). The SMC panel illustrates that most LMCa particles selected in that direction of the sky ( $b = -44.3^\circ$ ,  $l = 302.8^\circ$ ) are at  $\sim 58$  kpc from the Galactic center and have, on average, a radial velocity of  $\sim 5$  km/s, which is in excellent agreement with the observed SMC values (blue square).

The red vertical bands in the panels of Fig. 4 indicate a (generous) 20% uncertainty in the distance estimate to each dwarf; its intersection with LMCa particles is used to draw the velocity histograms in the right-hand side of each panel. Coincidence between the velocity of the blue square and the histogram indicates that the observed velocity is not unexpected in a scenario where the dwarf originates from a disrupted LMC group. The velocity histograms may therefore be used to “predict” the radial velocity of dwarfs for which kinematic data is not yet available, assuming a Magellanic origin.

As may be seen from Fig. 4, and not surprisingly, the SMC passes these tests handily, making its association with the LMC quite likely. On the other hand, the probability of association of a dwarf like Fornax is quite remote. Most debris in that direction of the sky are at much closer distances, and the little that overlaps in distance with Fornax (two particles) has a rather high positive radial velocity, quite unlike that observed. This illustrates the arguments used by S11 to exclude an LMC association not only for Fornax but also for all other Galactic satellites known at that time in case of first infall.

The 6 “new dwarfs” with kinematic data are shown in the bottom two rows of Fig. 4. From this comparison we conclude that Dra 2 has little chance of LMC association. Likewise, Ret 2, Tuc 2 and Gru 1 have velocities only marginally consistent with a Magellanic relation. Hy II, on the other hand, has the correct radial velocity for its distance, despite its large angular separation from the LMC, at the far northern edge region of the leading stream. The only clear candidate for Magellanic association is Hor 1, which is well within the expected velocity-distance range at its location.

### 3.3 Predicted radial velocities for candidate Magellanic satellites

We can use the procedure described in the previous subsection to predict the radial velocities that the remaining “new dwarfs” would

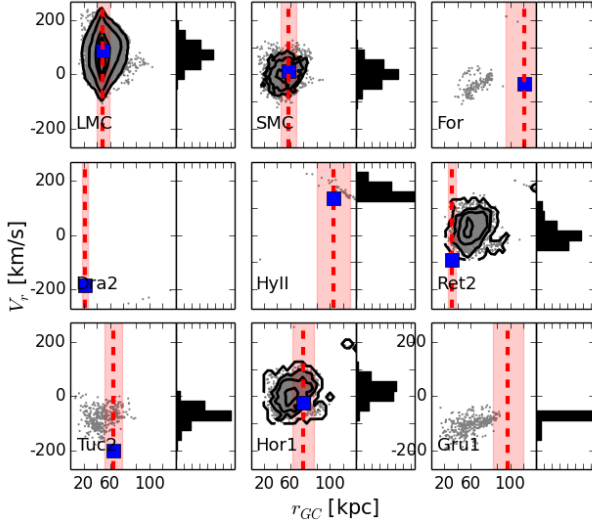


**Figure 4.** Galactocentric distance vs. radial velocity for LMCa particles within  $5^\circ$  from each observed dwarf (blue squares), as labeled. Particles with  $r_{GC}$  within 20% of the observed distance fall within the red shaded area, and are used to “predict” the radial velocity expected for LMC association (see black velocity histograms on the right of each panel). The top three panels are meant to illustrate the procedure for well studied systems. The LMC sits at the middle of the distribution *by construction*. The SMC is a likely LMC satellite; Fornax is not. The bottom two rows show the newly discovered dwarfs for which kinematic measurements are available. Only Hy II and Hor 1 show velocities consistent with those expected for prior association with the LMC.

have if they were truly Magellanic satellites. We show this in Fig. 5, which lists dwarfs in order of decreasing Galactic latitude. Inspection of individual panels suggests some preliminary conclusions. The Galactocentric distances measured for Pic 1 and Eri 2 seem inconsistent with previous association with the LMC. Cra 2 is in the same category, given the very little overlap with the edge of the leading arm of the stream. Aside from those three cases, all other dwarfs show some degree of overlap in the  $(l, b)$ - $r_{GC}$  plane with the LMCa debris. For the latter, the black histograms in Fig. 5 show their expected radial velocities for a Magellanic origin. We summarize these predictions in Table 3, together with uncertainties derived from the interquartile velocity range of the histograms in Fig. 5.

### 3.4 Probability of LMC association

The discussion of Figs. 4 and 5 suggests that, for each dwarf, the probability of prior LMC association scales with the total number of LMCa particles that match its sky position, distance, and radial velocity. We emphasize that these are not probabilities in the statistical “likelihood” sense, but nevertheless provide a simple way to rank order the dwarfs in terms of their potential association with the LMC and to weed out unrelated systems.

We adopt the following procedure, which attempts to quantify how likely the observed position (and velocity, when available) of a dwarf is, assuming LMCa membership. To this aim, we first compute, for each LMCa particle, the radius of a sphere,  $r_{100p}$ , that contains the 100 nearest debris particles, and rank them by this metric<sup>3</sup>. The smaller  $r_{100p}$  the more closely associated a particle

<sup>3</sup> We have checked that none of our conclusions change when selecting, instead, 50 or 200 particles for this exercise.

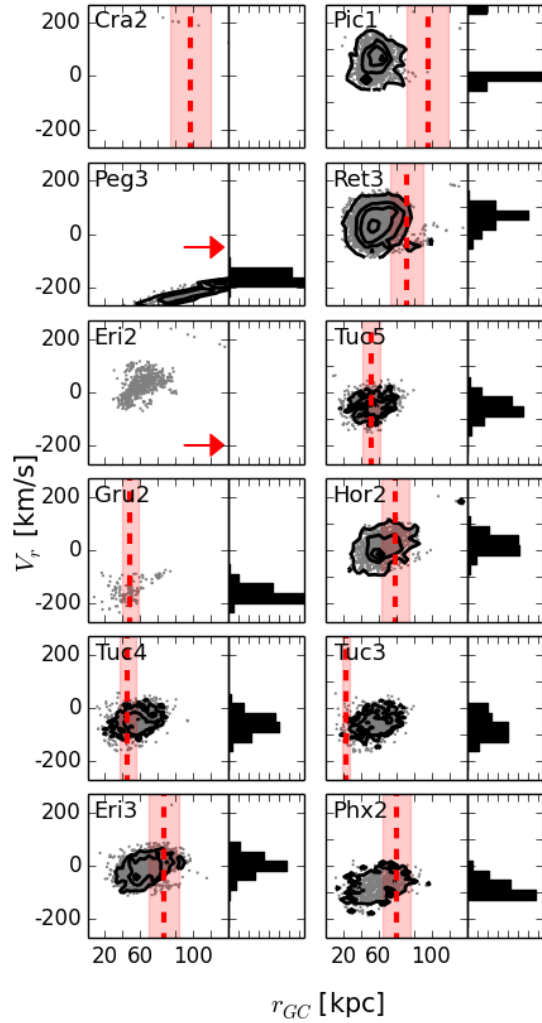


**Figure 5.** Same as Fig. 4 but for the new dwarfs with no measured  $V_r$ . The Galactocentric distances for Pic 1, Eri 2 and Tuc 3 seem inconsistent with the distances measured for the LMCa debris around their positions on the sky. On the other hand, Ret 3, Hor 2 and several of the Tucanas show high chance of association, at least based on their positions and distances alone.

is to the stream, which suggests that we may use  $r_{100p}$  to define a probability of association. In other words, we assign a dwarf a “probability of association” equal to the fraction of LMCa particles with  $r_{100p}$  values greater than that computed using the dwarf’s position. Probabilities assigned in this manner are listed in Table 1 for all newly-discovered dwarfs’.

For dwarfs with measured radial velocities, we compute a further probability by comparing its radial velocity with that of the nearest 100 LMCa particles. In practice, we use the mean and dispersion of those 100 radial velocities to compute the probability that the observed velocity of the dwarf was drawn at random from that distribution, assuming Gaussian statistics. The probabilities listed in columns 10 and 11 of Table 1 are computed by multiplying this value by that estimated using the position alone (columns 8 and 9, respectively).

The results are shown in Table 1, where we list all “new dwarfs”, as well as their assigned probability, with and without velocity information. As discussed before, aside from the SMC, the

procedure ranks Hor 1 as the best candidate for a true Magellanic satellite when considering satellites with or without radial velocities. Of systems without kinematic data, Hor 2, Eri 3 and Ret 3 are the best candidates, but this could certainly change when radial velocities become available. An example of the importance of kinematic information is provided by Ret 2, whose probability drops substantially (from  $\sim 0.10$  to  $0.01$ ) when adding its radial velocity to the analysis (assuming first pericenter).

We shall hereafter retain as “Magellanic candidates” systems whose probabilities exceed 50% that obtained for the SMC, without velocity information. The list of candidates is quite short: only 7 systems of the 20 new dwarfs make the cut in the case of position-only information: Hor 1, Hor 2, Eri 3, Ret 3, Tuc 5, Tuc 4 and Phx 2.

### 3.5 Second pericenter

The above procedure also allows us to explore the sensitivity of our findings to our assumption that the LMC is on first approach. We do this by performing the same analysis but using the LMCa data at second pericenter ( $t_{2p}$ ), after updating the Galactic coordinate system transformation described in Sec. 2.2. The new probabilities are also listed in Table 1.

Because of the procedure, probabilities are nominally higher, on average, at second pericenter. This is because the LMCa debris spreads out further in phase space at second pericenter, thus generally boosting the probability values computed for most systems. In general, however, there is a strong correlation between the probabilities at both pericenters, so our conclusions seem only weakly dependent on the assumption of first infall.

The increase in probability is most notable in the cases of Dra 2 and Hy II, whose probabilities jump from  $\sim 0.01$  and  $0.01$  in a first pericenter passage to  $0.50$ , and  $0.16$ , respectively, when considering the second pericentric passage. The jump in probability is even more remarkable when including velocities, reaching  $0.47$  in the case of Dra 2 at second pericenter, more than for the SMC.

The reason for this, in the case of Dra 2, is that it sits at the very far edge of the “trailing arm” of the tidal stream. Although its distance and velocity are consistent with an LMC association, at first infall there are only a few particles at that sky location and its probability is quite low. When the Clouds are in a second passage, several particles accumulate near the apocenter of the LMCa orbit, not far from where Dra 2 is, increasing substantially its probability of association. Similarly, Hy II is at the tip of the leading arm of the stream, a position that is much more heavily populated after the Clouds have completed one full orbit around the Galaxy.

### 3.6 Proper motions: conclusive proof of Magellanic origin

Ultimately, the most compelling evidence for LMC association will come from the proper motions of the new dwarfs. This is because all material associated with the LMC before infall is expected to retain the direction of its orbital angular momentum. In other words, to first order, Galactic tides are not expected to torque the LMC or its debris away from their original orbital plane.

We show this in Fig. 6, where we plot the *direction* of the orbital angular momentum of LMCa particles at first pericenter. The innermost and outermost isodensity contours enclose 5%, and 95% of all LMCa particles, respectively, and are centered at the location of the LMC orbital pole (central grey square). The other grey square (at  $b = -20^\circ$  and  $l = 175^\circ$ ) corresponds to the SMC, and is consistent with its assumed association with the LMC.

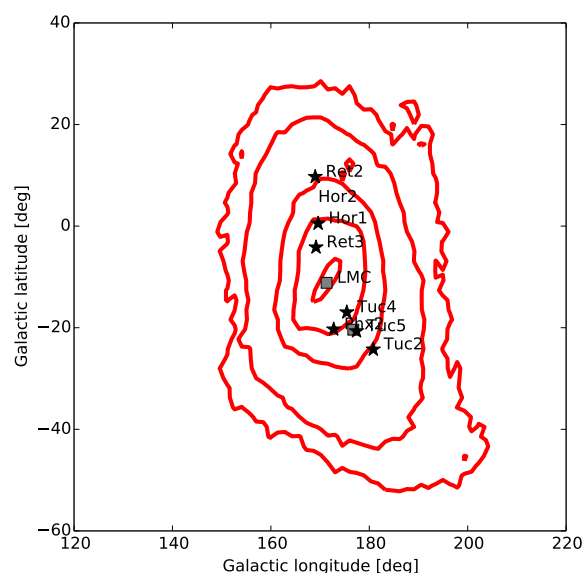


**Figure 6.** Sky coordinates of the orbital poles (i.e., the direction of the orbital angular momentum) of particles associated with LMCa. Contours show constant density lines for the distribution of all LMCa. Symbols correspond to the orbital poles estimated for new dwarf galaxies deemed likely candidate Magellanic satellites at first pericenter, as labeled. These estimates are based on the particles in the stream that are close in the sky and that lie at distances within 20% of the measured values (see shaded red regions in Fig. 4 and 5). The common infall scenario preserves the coherence of the orbital plane, resulting in a tight distribution of the orbital poles in a well-defined region of the sky.

We also show with starred symbols in Fig. 6 the orbital angular momentum direction predicted for each of the “candidate Magellanic satellites” (i.e., those that exceed 50% probability compared to the SMC) at first pericenter *assuming* that they were associated with the LMC. This is computed as the median  $l$  and  $b$  of the orbital poles of all LMCa particles with matching sky position and Galactocentric distance (i.e., the particles that fall into the red shaded regions of each panel in Figs. 4 and 5).

We list in Table 2, for each Magellanic candidate, the coordinates of the predicted orbital angular momentum unit vector, in a Cartesian system where the  $Z$ -axis is perpendicular to the Galactic disk, the  $X$ -axis points away from the sun and the  $Y$ -axis is defined such that we get a right-handed system. Uncertainties correspond to the r.m.s. values from the individual LMCa particles used for each dwarf.

Assuming a radial velocity (for those without a measurement), this is equivalent to predicting the tangential motion of each dwarf, which we also list in Table 3. The predicted projected velocities are shown with arrows in Fig. 2. Table 2 may therefore be used to evaluate the hypothesis of prior LMC association for these dwarfs once proper motions for these objects become available.

## 4 SUMMARY

We have used a  $\Lambda$ CDM cosmological N-body simulation of the formation of a Milky Way-sized halo to investigate which of the

20 newly-discovered Galactic satellites in the DES, Pan-STARRS, SMASH and ATLAS surveys might have been associated with the Magellanic Clouds before infall. Our study extends that of [Sales et al. \(2011\)](#), which used a massive subhalo with orbital parameters that closely match those of the LMC (an LMC analog: LMCa) and tracked the position and velocity of its constituent particles at first and second pericentric passages. This enables the probability of LMC association to be assessed by checking whether individual dwarfs lie in a region of phase space populated by debris from the disrupting LMC subhalo.

On the basis of that analysis, [Sales et al. \(2011\)](#) concluded that, except for the SMC, none of the other 26 Galactic satellites known at the time had positions and velocities consistent with a Magellanic origin. That was the first study to investigate a possible Magellanic association by using all of the available phase-space information in a fully cosmological context. Extending this study to the newly-discovered dwarfs yields the following conclusions, assuming that the LMC is at first pericentric passage.

- We eliminate four systems from our analysis. Sag 2, Eri 2, and Col 1 lie too far outside the LMCa footprint for their association with the LMC to be plausible. In addition, Ind 1 has recently been reclassified as a star cluster.

- For the rest of the systems, a quantitative “probability” of association has been computed using the positions and velocities of the LMCa particles closest to each dwarf. We deemed likely candidate Magellanic satellites dwarfs whose probability exceeds half the value assigned to the SMC.

- Of the six systems with available distances and radial velocities, only Hor 1 is clearly consistent with a Magellanic origin. Ret 2, Tuc 2, and Gru 1 have radial velocities which are only marginally consistent with LMC association. Dra 2 is too far off the LMCa first-pericenter footprint. Hy II has the right distance *and* radial velocity, but its probability is small, given its position at the thinly-populated, very far end of the LMCa leading tidal arm.

- Of the remaining 11 systems with only sky positions and distances, our analysis retains 6 of them at higher than 50% the probability of the SMC (Hor 2, Eri 3, Ret 3, Tuc 5, Tuc 4, and Phx 2). For these candidates, the nearest LMCa particles are used to *predict* their radial velocities, assuming a Magellanic origin.

- Aside from radial velocities, the most telling evidence of a potential LMC association would be provided by proper motions. These constrain the direction of the orbital angular momentum of each dwarf, which must roughly coincide with that of the LMC. We use this result to predict proper motions for all newly-discovered satellites, again assuming a Magellanic origin. The radial and tangential velocity predictions could be used to reassess the hypothesis of a possible Magellanic association once kinematic data become available.

Our conclusions are insensitive to our choice of first or second pericenter for the LMC, in the sense that the association probabilities of most dwarfs computed at each time show strong correlation. Because the LMCa debris spreads out to cover a larger volume in phase-space at second pericenter, the probabilities of four extra systems, computed using positions alone, are lifted above 50% that of the SMC: Tuc 2, Dra 2, Cra 2, and Peg 3. Of these, Tuc 2 seems quite unlikely given its radial velocity. Dra 2, on the other hand, has position and velocity consistent with being at the far end of the trailing stream during a second pericenter.

Our main conclusion is therefore that few of the newly discovered dwarfs are definitely associated with the LMC. This is not entirely unexpected. The simple scaling argument of [Sales et al.](#)

(2013) suggests that the fraction of all Galactic satellites associated with the Clouds should be close to the ratio of the stellar mass of the LMC and the Milky Way, i.e.,  $\sim 5\%$ . Given that we now have identified a total  $\sim 46$  dwarfs within 300 kpc from the Galactic center (excluding the LMC/SMC pair), only 2 to 3 should, in principle, be associated with the Clouds. So far our analysis seems consistent with this expectation. Accurate radial velocities and proper motions are needed to accept/reject the hypothesis of association between these dwarfs and the LMC. Confirming the existence of multiple Magellanic satellites would provide a wonderful confirmation of the hierarchical nature of galaxy formation predicted by the current cosmological paradigm.

## 5 ACKNOWLEDGMENTS

NK is supported by the NSF CAREER award 1455260. This research was supported in part by the National Science Foundation under Grant No. NSF PHY11-25915 and by the hospitality of the Kavli Institute for Theoretical Physics at the University of California, Santa Barbara.

## REFERENCES

- Bechtol K., Drlica-Wagner A., Balbinot E., Pieres A., Simon J. D., Yanny B., et al. 2015, *ApJ*, 807, 50
- Besla G., Kallivayalil N., Hernquist L., Robertson B., Cox T. J., van der Marel R. P., Alcock C., 2007, *ApJ*, 668, 949
- Boylan-Kolchin M., Springel V., White S. D. M., Jenkins A., Lemson G., 2009, *MNRAS*, 398, 1150
- Deason A. J., Wetzel A. R., Garrison-Kimmel S., Belokurov V., 2015, *MNRAS*, 453, 3568
- D’Onghia E., Fox A. J., 2015, *ArXiv e-prints* 1511.05853
- D’Onghia E., Lake G., 2008, *ApJL*, 686, L61
- Drlica-Wagner A., Bechtol K., Rykoff E. S., Luque E., Queiroz A., et al. 2015, *ApJ*, 813, 109
- Garrison-Kimmel S., Boylan-Kolchin M., Bullock J. S., Lee K., 2014, *MNRAS*, 438, 2578
- Jethwa P., Erkal D., Belokurov V., 2016, *ArXiv e-prints* 1603.04420
- Kallivayalil N., van der Marel R. P., Alcock C., Axelrod T., Cook K. H., Drake A. J., Geha M., 2006, *ApJ*, 638, 772
- Kallivayalil N., van der Marel R. P., Besla G., Anderson J., Alcock C., 2013, *ApJ*, 764, 161
- Kennedy R., Frenk C., Cole S., Benson A., 2014, *MNRAS*, 442, 2487
- Kim D., Jerjen H., 2015, *ApJL*, 808, L39
- Kim D., Jerjen H., Mackey D., Da Costa G. S., Milone A. P., 2015, *ApJL*, 804, L44
- Kim D., Jerjen H., Milone A. P., Mackey D., Da Costa G. S., 2015, *ApJ*, 803, 63
- Kirby E. N., Simon J. D., Cohen J. G., 2015, *ApJ*, 810, 56
- Koposov S. E., Belokurov V., Torrealba G., Evans N. W., 2015, *ApJ*, 805, 130
- Koposov S. E., Casey A. R., Belokurov V., et al. 2015, *ApJ*, 811, 62



**Table 1.** Parameters of the newly-discovered dwarfs considered in this paper, together with their probability of association with the LMC in either first or second pericenter passage, as defined in Sec. 3.4. Cols. 8 and 9 list probabilities computed using positions alone; cols. 10 and 11 also include also radial velocity data. We list the  $V$ -band absolute magnitude, stellar mass, galactocentric coordinates ( $l, b$ ), measured heliocentric velocity  $V_{\odot}$  and heliocentric distance  $D_{\odot}$  of each satellite, taken from the following references: [1] Koposov et al. 2015, [2] Drlica-Wagner et al. 2015, [3] Martin et al. 2015, [4] Laevens et al. 2015, [5] Kim & Jerjen 2015, [6] Kim et al. 2015, [7] Torrealba et al. 2016, [8] McConnachie 2012, [9] Simon et al. 2015, [10] Koposov et al. 2015, [11] Kirby et al. 2015, [12] Walker et al. 2016, [13] Martin et al. 2016). For cases without estimates of  $M_*$  we derive it from their listed  $V$ -band magnitudes assuming a mass-to-light ratio  $\gamma = 2$  in solar units. Dwarfs are grouped according to their probability of association with the Clouds at first pericenter, using only their distance and position on the sky (col. 8). The main two groups include “likely candidates” and “unlikely candidates”, according to whether their probabilities are above or below 50% the probability assigned to the SMC. The final group lists those that were discarded from the analysis, either because their position on the sky is such that the probability of LMC association is remote, or because they are considered star clusters, and not dwarf galaxies.

Name	$M_V$ [mag]	$M_*$ [ $10^3 M_{\odot}$ ]	$l$ [deg]	$b$ [deg]	$V_{\odot}$ [km/s]	$D_{\odot}$ [kpc]	Prob <sub>1st per</sub> ( $l, b, r$ )	Prob <sub>2nd per</sub> ( $l, b, r$ )	Prob <sub>1st per</sub> ( $l, b, r, V_r$ )	Prob <sub>2nd per</sub> ( $l, b, r, V_r$ )	Refs.
LMC	-18.1	$1.5 \times 10^6$	280.5	-32.9	262.2	51	0.63	0.71	0.52	0.53	[8]
SMC	-16.8	$4.6 \times 10^5$	302.8	-44.3	145.6	64	0.28	0.65	0.21	0.39	[8]
Hor 1	-3.4	1.96	270.9	-54.7	$112.8 \pm 2.5$	79	0.30	0.66	0.17	0.20	[1],[10]
Hor 2	-2.6	2.47	262.5	-54.1		26	0.27	0.59			[5]
Eri 3	-2.0	0.54	274.3	-59.6		87	0.25	0.64			[1]
Ret 3	-3.3	13.0	273.9	-45.6		92	0.25	0.66			[2]
Tuc 5	-1.6	9.	316.3	-51.9		55	0.15	0.46			[2]
Tuc 4	-3.5	4.	313.3	-55.3		48	0.15	0.35			[2]
Phx 2	-2.8	1.13	323.3	-60.2		83	0.15	0.55			[1]
Tuc 2	-4.4	4.9	327.9	-52.8	$-129.1 \pm 3.5$	69	0.11	0.47	0.06	0.06	[1],[12]
Gru 2	-3.9	5.0	351.1	-51.9		53	0.09	0.17			[2]
Ret 2	-2.7	1.0	265.9	-49.6	$62.8 \pm 0.5$	30	0.09	0.10	0.01	0.03	[1],[9],[10]
Tuc 3	-2.4	2.0	315.4	-56.2		25	0.08	0.10			[2]
Gru 1	-3.4	1.96	338.6	-58.8	$-140.5 \pm 2.0$	120	0.06	0.17	< 0.01	0.01	[1],[12]
Pic 1	-3.1	1.5	257.1	-40.4		114	0.06	0.09			[1]
Peg 3	-4.1	7.46	69.8	-41.8		26	0.05	0.32			[6]
Cra 2	-8.2	2.25	283.9	+41.9		118	0.02	0.41			[7]
Dra 2	-2.9	2.47	98.3	+42.9	$-347.6 \pm 1.8$	20	0.01	0.50	0	0.47	[4],[13]
Hy II	-4.8	7.1	295.6	+30.5	$303.1 \pm 1.4$	134	0.01	0.16	0.01	0.12	[3],[11]
Eri 2**	-6.6	37.3	249.4	51.4		380	0.0	0			[1]
Sag 2**	-5.2	2.47	189.0	-22.9		67	-	-			[4]
Ind 1**	-3.5	2.1	347.3	-42.6		100	-	-			[1]
Col 1**	-4.5	18.0	231.6	-28.9		182	-	-			[2]

Laevens B. P. M., Martin N. F., Bernard E. J., et al. 2015, *ApJ*, 813, 44  
 Lynden-Bell D., Lynden-Bell R. M., 1995, *MNRAS*, 275, 429  
 Martin N. F., Geha M., Ibata R. A., Collins M. L. M., Laevens B. P. M., Bell E. F., Rix H.-W., Ferguson A. M. N., Chambers K. C., Wainscoat R. J., Waters C., 2016, *MNRAS*, 458, L59  
 Martin N. F., Nidever D. L., Besla G., Olsen K., et al. 2015, *ApJL*, 804, L5  
 McConnachie A. W., 2012, *AJ*, 144, 4  
 Nidever D. L., Majewski S. R., Butler Burton W., Nigra L., 2010, *ApJ*, 723, 1618  
 Sales L. V., Navarro J. F., Cooper A. P., White S. D. M., Frenk C. S., Helmi A., 2011, *MNRAS*, 418, 648  
 Sales L. V., Wang W., White S. D. M., Navarro J. F., 2013, *MNRAS*, 428, 573  
 Shattow G., Loeb A., 2009, *MNRAS*, 392, L21  
 Simon J. D., Drlica-Wagner A., Li T. S., Nord B., Geha M., Bechtol K., et al. 2015, *ApJ*, 808, 95  
 Springel V., Wang J., Vogelsberger M., Ludlow A., Jenkins A., Helmi A., Navarro J. F., Frenk C. S., White S. D. M., 2008, *MNRAS*, 391, 1685  
 Springel V., White S. D. M., Frenk C. S., Navarro J. F., Jenkins A., Vogelsberger M., Wang J., Ludlow A., Helmi A., 2008, *Nature*, 456, 73

Springel V., Yoshida N., White S. D. M., 2001, *New Astronomy*, 6, 79  
 Torrealba G., Koposov S. E., Belokurov V., Irwin M., 2016, *ArXiv e-prints* 1601.07178  
 Tully R. B., Rizzi L., Dolphin A. E., Karachentsev I. D., Karachentseva V. E., Makarov D. I., Makarova L., Sakai S., Shaya E. J., 2006, *AJ*, 132, 729  
 Walker M. G., Mateo M., Olszewski E. W., Koposov S., Belokurov V., Jethwa P., Nidever D. L., Bonivard V., Bailey III J. I., Bell E. F., Loebman S. R., 2016, *ApJ*, 819, 53  
 Wetzel A. R., Deason A. J., Garrison-Kimmel S., 2015, *ApJ*, 807, 49  
 Wheeler C., Oñorbe J., Bullock J. S., Boylan-Kolchin M., Elbert O. D., Garrison-Kimmel S., Hopkins P. F., Kereš D., 2015, *MNRAS*, 453, 1305  
 Yozin C., Bekki K., 2015, *MNRAS*, 453, 2302

**Table 2.** Cartesian components of the direction (average) of the angular momentum of the LMCa particles near each Magellanic candidate dwarf, according to the discussion of Sec. 3.4. All vectors are normalized to have modulus unity. For each dwarf, we list the results for the first (top row) and/or second (bottom row) pericenter passage. The bottom group includes dwarfs that are only likely Magellanic candidates at second pericenter. Because the LMC is in a nearly polar orbit, the angular momentum of all material associated with it points in all cases in the  $-X$  direction (i.e., to the Sun from the Galactic center).

Name	time	$j_x$	$j_y$	$j_z$
LMC	$t_{1p}$	$-0.97 \pm 0.03$	$0.14 \pm 0.07$	$-0.19 \pm 0.10$
	$t_{2p}$	$-0.97 \pm 0.03$	$0.14 \pm 0.06$	$-0.18 \pm 0.09$
	observed	$-0.97 \pm 0.01$	$0.14 \pm 0.02$	$-0.18 \pm 0.03$
SMC	$t_{1p}$	$-0.92 \pm 0.05$	$0.04 \pm 0.10$	$-0.35 \pm 0.08$
	$t_{2p}$	$-0.90 \pm 0.05$	$0.05 \pm 0.17$	$-0.38 \pm 0.10$
	observed	$-0.91 \pm 0.05$	$0.08 \pm 0.11$	$-0.39 \pm 0.09$
Hor 1	$t_{1p}$	$-0.98 \pm 0.05$	$0.18 \pm 0.10$	$-0.04 \pm 0.09$
	$t_{2p}$	$-0.95 \pm 0.19$	$0.30 \pm 0.50$	$-0.10 \pm 0.36$
Hor 2	$t_{1p}$	$-0.97 \pm 0.02$	$0.24 \pm 0.09$	$-0.03 \pm 0.08$
	$t_{2p}$	$-0.73 \pm 0.18$	$-0.48 \pm 0.46$	$0.49 \pm 0.28$
Eri 3	$t_{1p}$	$-0.99 \pm 0.07$	$0.16 \pm 0.10$	$-0.04 \pm 0.07$
	$t_{2p}$	$-0.94 \pm 0.20$	$0.31 \pm 0.61$	$-0.14 \pm 0.37$
Ret 3	$t_{1p}$	$-0.98 \pm 0.02$	$0.18 \pm 0.07$	$-0.11 \pm 0.08$
	$t_{2p}$	$-0.94 \pm 0.19$	$0.28 \pm 0.50$	$-0.15 \pm 0.44$
Tuc 5	$t_{1p}$	$-0.93 \pm 0.03$	$0.12 \pm 0.13$	$-0.34 \pm 0.05$
	$t_{2p}$	$-0.90 \pm 0.04$	$0.09 \pm 0.14$	$-0.42 \pm 0.08$
Tuc 4	$t_{1p}$	$-0.95 \pm 0.03$	$-0.06 \pm 0.17$	$-0.30 \pm 0.06$
	$t_{2p}$	$-0.93 \pm 0.03$	$0.13 \pm 0.12$	$-0.28 \pm 0.08$
Phx 2	$t_{1p}$	$-0.93 \pm 0.02$	$0.13 \pm 0.10$	$-0.34 \pm 0.04$
	$t_{2p}$	$-0.92 \pm 0.02$	$0.13 \pm 0.13$	$-0.37 \pm 0.05$
Tuc 2	$t_{2p}$	$-0.87 \pm 0.03$	$0.08 \pm 0.16$	$-0.49 \pm 0.06$
Peg 3	$t_{2p}$	$-0.97 \pm 0.02$	$0.25 \pm 0.17$	$-0.03 \pm 0.12$
Cra 2	$t_{2p}$	$-0.97 \pm 0.08$	$0.12 \pm 0.17$	$0.20 \pm 0.16$
Dra 2	$t_{2p}$	$-0.81 \pm 0.08$	$-0.56 \pm 0.19$	$0.19 \pm 0.20$

**Table 3.** Predicted Galactocentric radial and tangential velocity for Magellanic candidate dwarfs under the assumption of association with the Clouds. We show the median and 25%-75% percentiles in the case of first (columns 2-4) and second (columns 5-7) pericenter passage. The last column shows the galactocentric radial velocity for the 6 dwarfs with measured kinematics. The bottom group includes dwarfs that are only likely Magellanic candidates at second pericenter.

Name	$V_r^{\text{pred}}$ [km/s]	$V_l^{\text{pred}}$ 1st per.	$V_b^{\text{pred}}$ 1st per.	$V_r^{\text{pred}}$ 2nd per.	$V_l^{\text{pred}}$ 2nd per.	$V_b^{\text{pred}}$ 2nd per.	$V_r^{\text{obs}}$ [km/s]
Hor 1	$19_{-22}^{+23}$	$5_{-30}^{+27}$	$330_{-25}^{+17}$	$23_{-17}^{+22}$	$1_{-38}^{+73}$	$266_{-200}^{+30}$	-23.2
Hor 2	$20_{-10}^{+25}$	$44_{-22}^{+26}$	$326_{-17}^{+19}$	$30_{-26}^{+36}$	$70_{-36}^{+13}$	$56_{-216}^{+21}$	
Eri 3	$5_{-23}^{+23}$	$-57_{-26}^{+78}$	$323_{-26}^{+22}$	$22_{-39}^{+31}$	$8_{-45}^{+65}$	$252_{-200}^{+28}$	
Ret 3	$72_{-32}^{+16}$	$36_{-15}^{+21}$	$326_{-19}^{+25}$	$38_{-23}^{+26}$	$-8_{-44}^{+86}$	$244_{-180}^{+35}$	
Tuc 5	$-58_{-21}^{+26}$	$-225_{-24}^{+27}$	$272_{-28}^{+23}$	$-50_{-27}^{+28}$	$-245_{-17}^{+30}$	$221_{-21}^{+32}$	
Tuc 4	$-58_{-21}^{+24}$	$-213_{-26}^{+25}$	$297_{-25}^{+23}$	$-43_{-18}^{+24}$	$-221_{-28}^{+18}$	$256_{-24}^{+24}$	
Phx 2	$-90_{-6}^{+30}$	$-273_{-8}^{+34}$	$180_{-5}^{+30}$	$-58_{-21}^{+24}$	$-237_{-18}^{+18}$	$161_{-25}^{+25}$	
Tuc 2	-	-	-	$-73_{-19}^{+29}$	$-265_{-23}^{+18}$	$133_{-33}^{+22}$	-201.5
Peg 3	-	-	-	$-110_{-16}^{+8}$	$-16_{-9}^{+10}$	$-131_{-8}^{+7}$	
Cra 2	-	-	-	$108_{-21}^{+36}$	$-156_{-36}^{+49}$	$228_{-42}^{+16}$	
Dra 2	-	-	-	$-189_{-5}^{+16}$	$104_{-17}^{+36}$	$-265_{-4}^{+14}$	-185.1